STARS

1-1-1997

Work function determination of zinc oxide films

K. B. Sundaram
University of Central Florida

Ashamin Khan
University of Central Florida

Recommended Citation

Sundaram, K. B. and Khan, Ashamin, "Work function determination of zinc oxide films" (1997). *Faculty Bibliography 1990s*. 2110.
https://stars.library.ucf.edu/facultybib1990/2110

Work function determination of zinc oxide films

K. B. Sundaram, and Ashamin Khan

Work function determination of zinc oxide films

K. B. Sundaram[a)] and Ashamin Khan[b)]

Department of Electrical and Computer Engineering, University of Central Florida, Orlando, Florida 32816-2450

Zinc oxide-silicon heterojunctions were fabricated using both *n*- and *p*-type silicon. The zinc oxide films were deposited by the magnetron sputtering process at various substrate temperatures to form these devices. The electrical properties of these devices were measured and the work function of the zinc oxide was evaluated from these properties. © *1997 American Vacuum Society.*
[S0734-2101(97)03102-3]

I. INTRODUCTION

Zinc oxide (ZnO) is an *n*-type wide band-gap semiconductor that has potential application as a material for optoelectronic devices. Thin films of zinc oxide have been widely studied as a piezoelectric material for surface acoustic wave devices.[1,2] Low-loss optical wave guides have been fabricated using epitaxial ZnO films.[3] An electro-optic modulator was also reported using ZnO films.[4] Zinc oxide film has been used as a top contact window layer for solar cell applications due to its high optical transparency and electrically conducting nature.[5–7] ZnO films have a high infrared reflectance and high visible transmittance. Presently indium tin oxide (ITO) layers are used as energy efficient windows for solar cells and liquid crystal displays. The components of ITO, namely, In and Sn, are limited in supply and are more expensive than zinc. Further, for the fabrication of amorphous-silicon (*a*-Si) solar cells, ITO coated glass substrates are used. The *a*-Si films are deposited onto the ITO layer by the plasma enhanced chemical vapor deposition (PECVD) process. During this deposition, ITO films are exposed to hydrogen plasma that reduces the metal oxide optical transparency. In and Sn based conducting layers are not wise to use for low cost solar cells. ZnO films are more stable than ITO based films in the presence of H_2 plasma. In addition, zinc is a cheap, abundant, and nontoxic element. Although the optical and electrical properties of zinc oxide have been studied extensively, there is no report of the work function of zinc oxide films. In the present work, ZnO–Si heterojunctions were fabricated and their electrical properties were measured. The work function of zinc oxide films was evaluated from these properties.

II. EXPERIMENT

Zinc oxide/silicon heterojunctions were prepared using both *n*- and *p*-type wafers. All the samples were (100) silicon single-crystal wafers polished on one side only. The resistivities of the *p*-type samples were 10 and 23 Ω cm where as the resistivity of the *n*-type was 5 Ω cm. The wafers were cut into pieces 1.5 cm long by 1 cm wide. The wafers were cleaned with boiling trichloroethane, acetone, and methanol and then dipped in 1:1 H_2SO_4:H_2O_2 for 3 min. Subsequently the wafers were etched with a buffered oxide etch (BOE) ($13NH_4F$:2HF) diluted with water for 3 min to remove any surface oxide. Finally the wafers were washed with deionized water and this was followed by blowing dry with nitrogen. To provide low resistance electrical contacts (ohmic contacts) to *p*-type Si, a 300-nm-thick aluminum layer was deposited onto the back side of the wafer. For *n*-type Si a phosphorus doped nickel layer was deposited by the electroless plating method.[8] The samples were annealed at 450 °C for 30 min for alloying in an argon ambient in order to get good ohmic contacts. Before deposition of the ZnO film, the front of the sample was etched in a BOE while masking the back side with Apiezon wax. The wax was removed with trichloroethylene and the wafers were cleaned and dried.

ZnO films were deposited in a radio frequency (rf) magnetron sputtering system (US Gun II) using a 5-cm-diam pressed zinc oxide target (99.999% purity, Angstrom Sciences). The samples were placed into the system along with a metal shadow mask to form 1–2-mm-diam dots of ZnO onto the Si. The target to substrate distance was 3.2 cm. The system was evacuated to a pressure of 5×10^{-6} Torr while the substrate was heated. The base pressure in the system was adjusted with a throttle valve to maintain it at 20×10^{-3} Torr during deposition with an argon flow of 5 sccm. Before initiating the deposition onto the substrates, the target was precleaned for 15 min. The ZnO films were deposited at different substrate temperatures ranging from 50 to 250 °C. The rf power used was 150 W and the films were deposited for 30 min. Film thickness ranged from 250 to 300 nm.

The $I-V$ characteristics of the fabricated diodes were measured using a Hewlett Packard semiconductor parameter analyzer (model HP4145B). All measurements were taken under dark conditions. Both the $I-V$ characteristics and the $\log I-V$ were plotted using the semiconductor parameter analyzer.

III. RESULTS AND DISCUSSION

The deposited zinc oxide films showed typical resistivity of nearly 10^{-2} Ω cm. Both the ZnO/*n*-Si and the ZnO/*p*-Si junctions showed good rectifying characteristics. In the ZnO/*n*-Si junction, Si is negative for forward current, while the
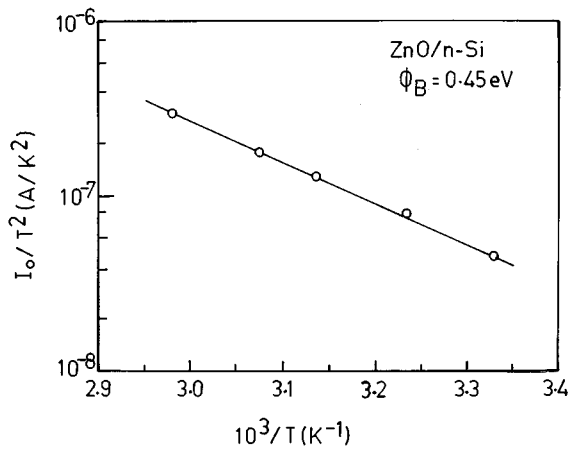
FIG. 1. Semi-log plot of I_0/T^2 vs $10^3/T$ for ZnO/n-Si heterojunctions.
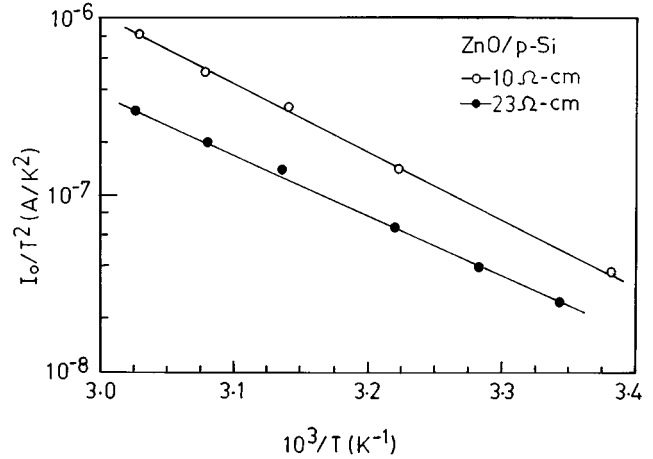
FIG. 2. Semi-log plot of I_0/T^2 vs $10^3/T$ for ZnO/p-Si heterojunctions.

ZnO/p-Si junction requires positive voltage on the Si for the forward bias condition. The forward biasing conditions are very similar to metal/n-Si and metal/p-Si Schottky barrier contacts. The room temperature reverse saturation current (I_0) of the diodes was obtained by extrapolating the reverse current region of the log I–V plots. Because of the high conductivity of the ZnO films, it is assumed that the Fermi level coincides with the conduction band edge in the ZnO. Under this assumption, the electron affinity and the work function of ZnO are nearly equal. The transition region is predominantly on the Si side for the junction. The discontinuity in the conduction band edge, ΔE_c, is equal to the difference in the electron affinities between ZnO and Si. In this context, the predominant current mechanism is assumed to be Schottky emission of carriers over the potential barrier for both n- and p-type heterojunctions. The reverse saturation current density is of the form[9]

$$J_0 = I_0/A = A^* T^2 \exp(-\phi_B/kT), \qquad (1)$$

where I_0 represents the reverse saturation current, A is the junction area, A^* is the Richardson constant, ϕ_B is the Schottky barrier height, k is the Boltzman constant, and T is temperature in kelvin. Semi-log plots of I_0/T^2 vs $10^3/T$ were plotted for devices with n- and p-type substrates. ϕ_B was found from the slope of the line. Figure 1 shows the plot for ZnO/n-Si heterojunctions from which ϕ_{Bn} was found to be 0.45 eV. Figure 2 shows similar plots for ZnO/p-Si junctions with Si resistivities of 10 and 23 Ω cm, respectively. Here, ϕ_{Bp} values were found to be 0.72 and 0.69 eV, respectively, for the above samples of Fig. 2. Based on the simple Schottky–Mott model, the work function Φ_m of ZnO was calculated using the relation of $\Phi_m = X_{Si} + \phi_{Bn}$, for the junction with n-Si and $\Phi_m = E_g + X_{Si} - \phi_{Bp}$ for p-Si, where X_{Si} and E_g are the electron affinity and band gap of silicon having values of 4.05 and 1.12 eV, respectively.[9] The work function values for ZnO ranged from 4.45 to 4.5 for the fabricated devices. This work function value is close to the value reported for the defect free ZnO ($10\bar{1}0$) single crystals by Göpel et al.,[10] Further, $\phi_{Bn} + \phi_{Bp}$ gives a value of 1.155 eV that is very close to the band gap of Si.

Prior to ZnO deposition, the Si surface was chemically cleaned and this process invariably leaves a thin (1–2 nm) insulating oxide layer on the semiconductor surface. Because of the presence of an insulating layer between Si and ZnO, according to the Bardeen model the barrier heights ϕ_{Bn} and ϕ_{Bp} are modified approximately and are given by[9]

$$\phi_{Bn} = C(\Phi_m - X_{Si}) + (1 - C)(E_g - \phi_0), \qquad (2)$$

where

$$C = \frac{\epsilon_i}{\epsilon_i + q^2 \delta D_s},$$

where δ the thickness of the oxide layer, and ϵ_i its total permittivity. The surface states are assumed to be distributed in energy within the band gap, with density of states D_s/cm^2. The position of neutral level ϕ_0 is measured from the top of the valence band. A similar analysis for the case of a p-type semiconductor shows that ϕ_{Bp} is approximately given by

$$\phi_{Bp} = C(E_g - \Phi_m + X_{Si}) + (1 - C)\phi_0. \qquad (3)$$

For a given interfacial layer thickness, $(\phi_{Bn} + \phi_{Bp}) \approx E_g$, owing to the similarity of the surface states in p- and n-type Si.

Using the data from the previous work by Turner and Rhoderick for their metal/n-Si Schottky barriers[11] with $qD_s = 2 \times 10^{12}$/cm^2 for n-Si, $\delta = 1.5$ nm, and $\epsilon_i = 3.9$, $\phi_0 = 0.27$ eV, and assuming the work function of ZnO to be around 4.5 eV as calculated above in our experiment, ϕ_{Bn} was calculated using Eq. (2) and was found to be 0.49 eV. The range of δ taken corresponds to the range over which the model can be reasonably expected to hold, i.e., tunneling can take place through the interfacial layer, the parasitic resistance of which can be taken as zero. Similarly, using the data from previous work by Smith and Rhoderick[12] with $qD_s = 3 \times 10^{12}$/cm^2 for p-Si, and $\phi_0 = 0.33$ eV, ϕ_{Bp} was calculated using Eq. (3) and was found to have a value of 0.61 eV. Therefore, assuming the presence of an insulating layer between ZnO and Si, ϕ_{Bn} increased and ϕ_{Bp} decreased compared with the conventional Schottky–Mott model approach. Deposition of ZnO at higher temperatures will cause growth
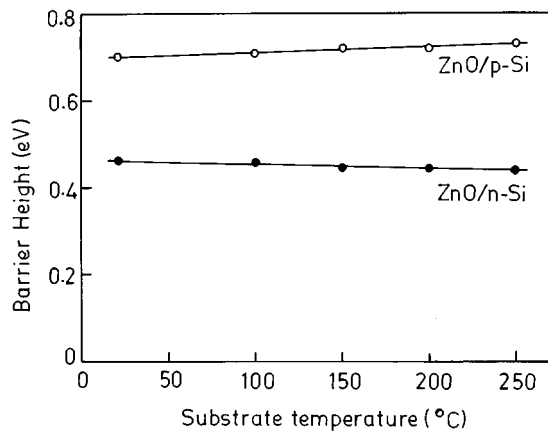
FIG. 3. Barrier height as a function of substrate deposition temperature.

of the oxide and a subsequent reduction in the density of states. Based on Eqs. (2) and (3), this reduction in the density of states will cause a decrease in ϕ_{Bn} for the n-Si device and an increase in ϕ_{Bp} for p-Si. A similar trend was observed with only small changes in the barrier heights for both ZnO/n-Si and ZnO/p-Si junctions prepared by depositing ZnO at higher substrate temperatures and is shown in Fig. 3. Again, $\phi_{Bn} + \phi_{Bp}$ corresponds approximately to E_g of Si. Deposition at higher temperature will increase oxygen diffusion towards the Si interface and this will make ZnO less stoichiometric due to a greater oxygen deficiency. More oxygen defects in ZnO will correspond to a reduced work function of

ZnO. This work function reduction will decrease ϕ_{Bn} and increase ϕ_{Bp} based on the above equations. The same trend is seen in Fig. 3. A similar reduction in work function was observed by Göpel et al. when the ZnO single crystal had more defects.[10]

IV. CONCLUSIONS

The work function of sputter deposited ZnO films was obtained from the electrical properties of ZnO/p-Si and ZnO/n-Si junctions. The estimated values of the work function based on the Schottky barrier model showed values between 4.45 and 4.50 eV for the films. These values were also interpreted by assuming the presence of a very thin SiO_2 layer at the interface of ZnO and Si.

[1] F. S. Hickernell, IEEE Trans. Sonics Ultrason. **32**, 621 (1986).
[2] S. Maniv and A. Zangvil, J. Appl. Phys. **52**, 2787 (1978).
[3] M. Wu, A. Azuma, T. Shiosaki, and A. Kawabata, J. Appl. Phys. **62**, 2482 (1987).
[4] D. Persegol, E. Pic, and J. Plantier, J. Appl. Phys. **62**, 2563 (1987).
[5] N. G. Dhere, Thin Solid Films **193–194**, 757 (1990).
[6] J. Aranovich, A. Ortiz, and R. H. Bube, J. Vac. Sci. Technol. **16**, 994 (1979).
[7] J. Hu and R. G. Gordon, J. Electrochem. Soc. **139**, 2014 (1992).
[8] M. V. Sullivan and J. H. Eigler, J. Electrochem. Soc. **104**, 226 (1957).
[9] S. M. Sze, *Physics of Semiconductor Devices*, 2nd ed. (Wiley, New York, 1981), pp. 256 and 270.
[10] W. Göpel, L. J. Brillson, and C. F. Brucker, J. Vac. Sci. Technol. **17**, 894 (1980).
[11] M. J. Turner and E. H. Rhoderick, Solid-State Electron. **11**, 291 (1968).
[12] B. L. Smith and E. H. Rhoderick, Solid-State Electron. **14**, 71 (1971).